DIGITAL ANALYSIS OF ACTIN FILAMENTS IMAGES OBTAINED BY FLUORESCENCE MICROSCOPY

C.M. RUSU[#], MIHAELA BACALUM*, ANTONIA TEONA DEFTU**, BEATRICE MIHAELA RADU**, M. RADU**

*Department of Life and Environmental Physics, "Horia Hulubei" National Institute of Physics and Nuclear Engineering, 30, Reactorului st, Măgurele, Romania, [#]e-mail: calinmircea@gmail.com
**Department of Anatomy, Animal Physiology and Biophysics, Faculty of Biology, University of Bucharest, 91–95, Splaiul Independenței, Bucharest, Romania

Abstract. The actin cytoskeleton is a basic determinant of cellular morphology and motility. Actin cytoskeleton study is important because a wide spectrum of cellular processes can be monitored through the conformational changes that occur at its level. A template-based method for linear detection was used to process and perform a quantitative analysis of cytoskeleton morphology in various cell types. This approach is fitted for a precise calculation of various parameters such as fiber length and cytoskeleton polarization, and can be used to follow the changes in the morphology of the actin cytoskeleton due to physiological modifications. In our study, several images of four different cell lines: bEnd.3, BJ, MG-63 and OLN-93 were analyzed in control conditions, in order to assess the structural organization of the actin cytoskeleton. A comparative analysis was also performed on the robustness and adaptability of the proposed algorithm, using the images of the four cell lines. The aim of this study was to establish how well the program recognizes the fibers apart from other cellular structures and debris. Following the analysis, criteria were set for the adjustment of computational parameters (e.g., angular resolution, kernel matrix size, etc.). The use of the segmentation algorithm provided consistent quantitative information, revealing the distributions of important morphological features. The adaptive character of the method, due to the manipulation of computational parameters, enables an efficient segmentation of the microscopy images. Thus, a high precision quantitative analysis of the microscopy images was performed, for the assessment fiber morphology and determination of the optimal set of computational parameters used for the digital extraction of the fibers.

Key words: cytoskeleton, actin, microscopy, confocal, digital, analysis.

INTRODUCTION

Many of the most recent advances in cellular biology were possible due to the development of higher resolution microscopy techniques such as confocal microscopy, super-resolution fluorescence microscopy, etc. These increased capabilities facilitate the better study of intracellular structures. However, certain intracellular structures,

Received: September 2018;
in final form September 2018.

ROMANIAN J. BIOPHYS., Vol. 28, No. 4, P. 147–157, BUCHAREST, 2018

such as the cytoskeleton, demand a rather quantitative view, for the better understanding of dynamics underlying their broad conformational variation.

The cytoskeleton is the largest cellular organelle and the main facilitator of cell migration. The cytoskeleton of eukaryotic cells is constituted of microtubules, intermediate filaments and microfilaments. Microfilaments, also known as actin filaments, are the narrowest in diameter (~7 nm).

The cytoskeleton can easily induce changes in the cell morphology through assembling and disassembling. Unlike other organelles, the size of the cytoskeleton varies and its fibers have the tendency to form complex structures [1]. To detail, the shape and size of the actin fibers are variable between different cell lines, providing a mean of structural and functional characterization. These differences range from fiber length and orientation to pattern complexity and structural polarization.

Physiological changes can also be observed through specific modifications of the actin filaments organization [7]. To date, actin filaments have been described to be keyplayers in various physiological processes, including motility, division, morphogenesis, cell-shape regulation, and mechanosensation [8].

Some of the morphological changes that occur at the level of the actin filaments cannot be precisely observed from unprocessed microscopy images due to the limitations of the optical microscopes. Also, standard image analysis techniques are not robust against smaller structure modifications [5], and therefore an efficient characterization of different cell lines, in variable conditions, would not be possible.

Computational methods, based on pattern recognition and synthetic structure filtering, were developed in order to quantify specific actin fibers network characteristics, such as fiber length or cytoskeleton polarization. Such information can be easily obtained following the digital processing of the images. While standard methods, such as mathematical intensity subtraction or binary thresholding, are efficient for the detection and segmentation of organelles with less morphological variability, the actin fibers require a more specific detection method [2]. The FiberScore algorithm, developed by Nurit Lichtenstein, provides a reliable tool for fiber-like patterns detection and segmentation, being robust against noise and unevenly distributed intensities [3]. A complete characterization of different cell lines, based on the FiberScore algorithm, can be consistent against different morphologies and cell types, as the method can establish strong quantitative criteria of classification. Thus, the aim of this study was to optimize the FiberScore algorithm and to check if we can differentiate in terms of actin fibers morphology between control conditions of different cell lines. We first established a reliable set of computational parameters for an optimal detection of fibers, independent of the cell line or culture conditions. Following, we applied the optimized FiberScore algorithm, to four different cell lines (bEnd.3, BJ, MG-63, and OLN-93) and we obtained quantitative data regarding: fiber polarization, total fiber length, mean fiber length and number of fibers for images of individualized cells. Our data indicates that an efficient differentiation of cellular morphology can be achieved through the analysis of actin fiber geometry and optimal adjustment of computational parameters.

MATERIALS AND METHODS

CELL LINES

bEnd.3 (ATCC, USA), transformed mouse endothelial cells from the cerebral cortex, were cultured in Advanced Dulbecco Modified Eagle's Medium (Advanced DMEM), supplemented with 10% fetal bovine serum FBS. Human osteosarcoma MG-63 cells (ECACC, UK) were grown in Modified Eagle Medium (MEM) supplemented with 2 mM L-glutamine, 10% FCS and 1% non-essential amino acids (complete medium, Sigma). OLN-93 cells were provided as a gift from Prof. Marcel Ameloot (University of Hasselt, Belgium), with the agreement of Dr. C. Richter-Landsberg (Department of Biology, Molecular Neurobiology, University of Oldenburg, Germany). The cells were grown in DMEM supplemented with 1% FBS and on coverslips coated with 40 μg/mL PLL (poly-L-lysine) to ensure cell differentiation. Human foreskin fibroblasts BJ cells (ATCC, USA) were cultured in MEM supplemented with 10% FBS. To all media were added 100 units/mL of penicillin and 100 μg/mL of streptomycin. Cells were grown at 37 °C in a humidified incubator under an atmosphere containing 5% CO_2. Cell cultivation media and reagents were purchased from Biochrom AG (Berlin, Germany). For microscopy recordings cells were seeded on 10 mm coverslips at a density of 40,000 cells per 3.14 cm^2 for bEnd.3, 32,000 cells per 3.14 cm^2 for MG-63, 20,000 cells per 3.14 cm^2 for BJ for 24 h and 1,000 cells per 3.14 cm^2 for OLN-93 for 48 h.

PHALLOIDIN STAINING AND CELL IMAGING

Cytoskeleton actin filaments were stained with phalloidin-FITC (Phalloidin, Fluorescein Isothiocyanate Labeled, Sigma-Aldrich, USA) according to the manufacturer protocol. Briefly, cells were washed with PBS (5 min, three times), fixed for 5 min with 3% paraformaldehyde, washed with PBS, permeabilized with 0.1% Triton X-100 in PBS, washed with PBS, stained with 20 μg/mL phalloidin-FITC at room temperature for 1 h, washed with PBS and mounted and sealed on glass slides with FluorSave™ Reagent (Merck Millipore, Germany).

The fluorescence images were acquired using an Andor DSD2 Confocal Unit (Andor, Ireland) mounted on an Olympus BX-51 (Olympus, Germany) epifluorescence microscope equipped with a 40x objective and an appropriate GFP/FITC filter cube (excitation filter 466/40 nm, dichroic mirror 488 nm and emission filter 525/54 nm).

THE SEGMENTATION ALGORITHM

The FiberScore algorithm, implemented by Lichtenstein *et al.*, is used for the precise segmentation and quantification of actin fibers from confocal microscopy

images, through the variation of computational parameters. The detection of actin fibers is determined by the probability of a pixel neighborhood to belong to a fiber structure. This probability is computed through the correlation of pixel regions in the analyzed image with synthetic fiber-like digital pixel structures at different angles [2].

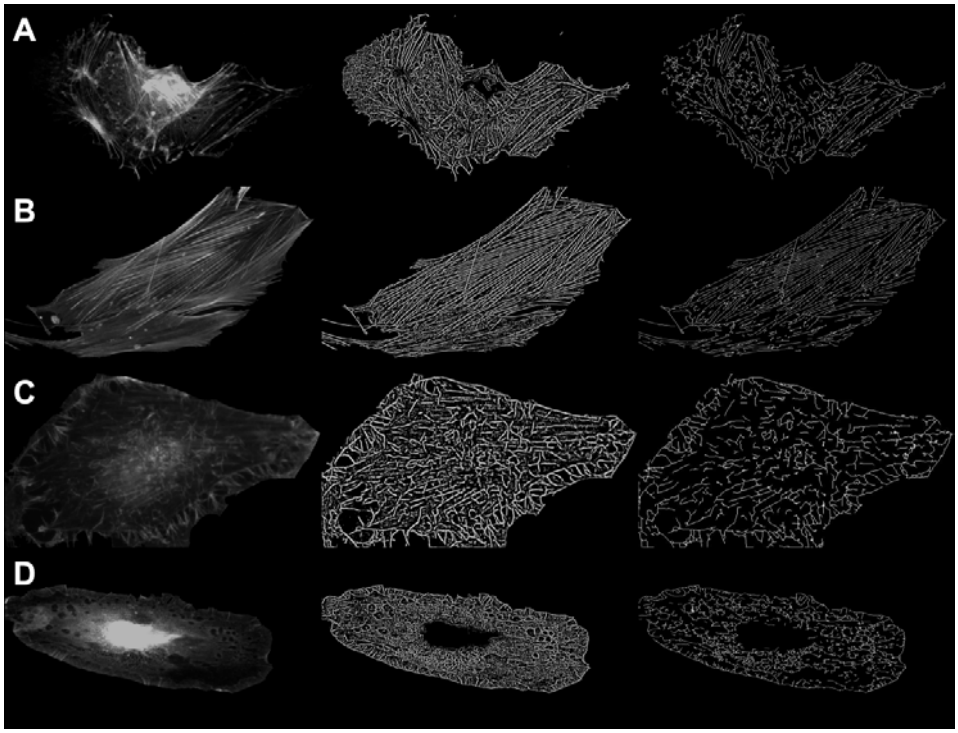

Fig. 1. Steps of the image processing performed with the FiberScore algorithm (left column – original image, middle column – convolution image, right column – thinned image) applied to (A) bEnd.3 cells, (B) BJ cells, (C) MG-63 cells, and (D) OLN-93 cells.

The synthetic fiber-like structure is represented by an n-dimensional raster of pixels, generated through a Bresenham's line algorithm [4]. The pixels of this specific raster are selected in order to form a straight line between two given points. A close approximation of an actin fiber is therefore established, taking into account the length and the orientation angle of the pixelated line. The intensities along the line are weighted by a Gaussian profile. Using the linear structure generated, a kernel matrix, with the pixel of interest in the center, is defined. For each central pixel of interest, a correlation coefficient at a specific angle is calculated using the intensity of the pixel in the actual image and the mean intensity along the pixelated line.

As the entire image is weighted by the kernel matrix, a convolution mask is created. The mask is comprised of the pixels that exceeded a preset threshold for the correlation coefficient. After the application of the filter, the original image is segmented, highlighting only the actin fibers (Fig. 1). For the quantitative analysis the mask is thinned (Fig. 1), reducing the fibers to a width of one pixel [2]. Also, we changed the color scheme of every image to binary, in order to keep the quantitative analysis independent of the pixel intensity.

The segmentation was carried out for confocal microscopy images, each containing a single isolated and individualized cell. The contrast and brightness levels were adjusted prior to the processing, for a more efficient detection.

THE COMPUTATIONAL PARAMETERS

The adjustable computational parameters are a series of threshold values used for the generation of the convolution mask and the thinned mask. The parameters used for the actual detection of fibers are the size of the kernel matrix and the angular resolution [2]. The size of the kernel matrix has to be an integer and was originally defined by Lichtenstein [2] to have the value of 6. The angular resolution defines the step size of the angle at which the correlation coefficient is computed. For an accurate detection, we set a higher angular resolution (*ang. res*. = 10 steps of 9°) than the one used in the original algorithm (*ang. res.* = 3 steps of 30°). This step proved to be robust against the variations in the fiber orientations between cell lines.

The minimum threshold for accepted correlation coefficient is used for the prevention of debris or false fiber detection. Also, minimum threshold values for the standard deviations along the fiber structures and between two fibers are defined. These two parameters are used for removing false detections in areas with a greater number of fibers [2].

A threshold is also defined for the pixel intensity values. This parameter is used for removing the background around the fiber structures. In the program developed by R. Pham, based on the FiberScore algorithm, the values for this parameter were normalized, so that they can be set ranging from 0 to 1 [3].

A minimum accepted fiber length is set prior to the thinning of the convolution mask, preventing the detection of unwanted linear structures resulting from labeling errors.

For this study, we choose to use the same set of parameters for each set of images (Table 1). However, an exception was made for the minimum accepted fiber length, which was varied to assure the accurate detection of fibers even for smaller and less organized cells. We used a minimum fiber length of 15 pixels for the bEnd.3 and BJ cells and a smaller value of 10 pixels for MG-63 and OLN-93 cells.

Table 1

Adjustable computational parameters

Size of the kernel matrix	6 (pixels)
Angular resolution	10 (steps of 9°)
Threshold for correlation coefficient	0.1
Threshold for normalized standard deviation	0.07
Threshold for normalized standard deviation between fibers	1.2
Minimum threshold for image intensity values	0.3

THE QUANTITATIVE ANALYSIS

We used the processed images resulted from the FiberScore algorithm to perform a quantitative analysis of the cytoskeleton morphology. Several values of interest were computed, such as: number of fibers, total fiber length, mean fiber length and cytoskeleton polarity.

The number of fibers and total fiber length were computed by counting the pixels forming the thinned mask and the isolated fiber structures detected above the minimum fiber length threshold. Mean fiber length is defined as the ratio between the total length and the number of fibers.

The cellular polarity is the asymmetric organization of several cellular components including plasma membrane, cytoskeleton or cellular organisms [9]. The cytoskeleton polarity values were computed using the formula from the original FiberScore algorithm [2]:

$$D = \sqrt{D_x^2 + D_y^2} \tag{1}$$

where D_x and D_y are the cos and sin of the direction of the fiber structure with the highest correlation coefficient, in each pixel of the thinned mask. The polarity value ranges from 0 (highly unorganized cytoskeleton) to 1 (perfectly organized cytoskeleton) (Fig. 2).

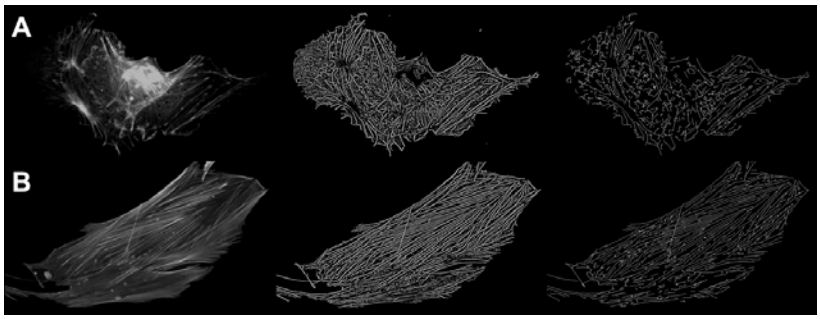

Fig. 2. Comparison between higher and lower polarity values (left column – original image, middle column – convolution image, right column – thinned image): (A) bEnd.3 cell with polarity value of 0.036 and (B) BJ cell with polarity value of 0.52.

STATISTICAL ANALYSIS

The parameters calculated are represented as mean ± standard deviation if not otherwise stated. The p-value of <0.05 is considered statistically significant. The comparison between the four cell types was carried out using the one-way analysis of variance (ANOVA), and the multiple means comparison was performed using the Fisher post-hoc test. The error bars show the standard deviation and the significance labeling following the post-hoc test is in the form of: *$p < 0.05$; **$p < 0.01$; ***$p < 0.005$; ****$p < 0.001$.

RESULTS AND DISCUSSION

FIBER LENGTH

A comparative analysis of total fiber length of individual cells, number of fibers and mean fiber length was performed (Figs. 3–5). Individual fiber lengths are determined by counting the pixels in every image of individualized cells, with the thinned mask applied. The number of fibers is determined by counting the pixelated linear structures (fibers) that formed the thinned mask and the mean fiber lengths are determined by dividing the total fiber length by the number of fibers detected for each cell.

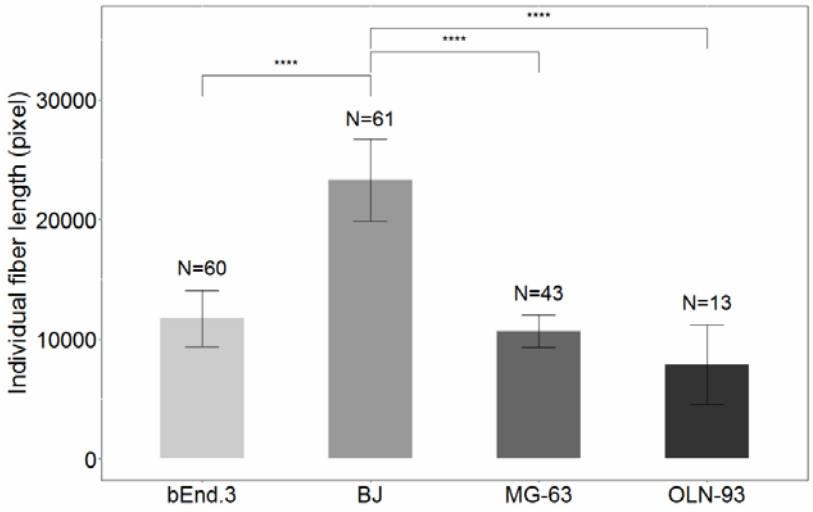

Fig. 3. Individual fiber length determined for the four types of cells. *N* represents the number of cells analyzed for each condition. The data were analyzed using one-way ANOVA with Fisher post-hoc tests with significance level: *$p < 0.05$; **$p < 0.01$; ***$p < 0.005$; ****$p < 0.001$.

The evaluation of individual fiber lengths shows significant differences between BJ cells and the other cell lines (Fig. 3). However, there are no significant differences between individual fiber lengths of the other three cell types.

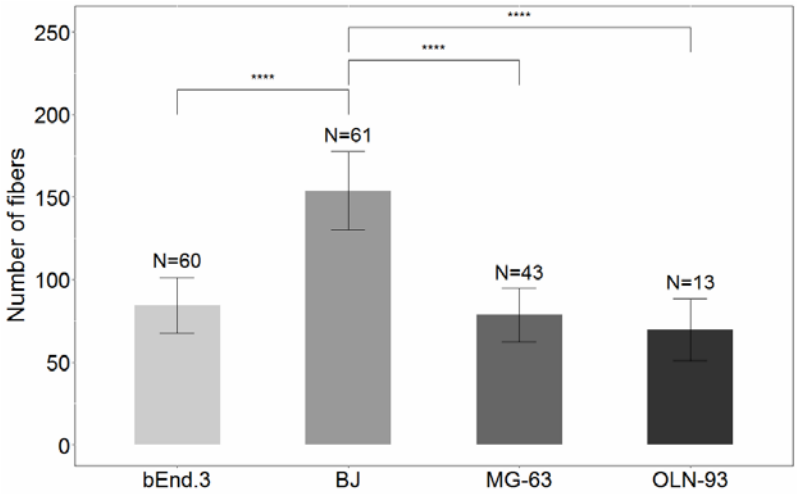

Fig. 4. Number of fibers determined for the four types of cells. *N* represents the number of cells analyzed for each condition. The data were analyzed using one-way ANOVA with Fisher post-hoc tests with significance level: *$p < 0.05$; **$p < 0.01$; ***$p < 0.005$; ****$p < 0.001$.

In Fig. 3 we can see that the number of fibers detected for BJ cells were around 150 per cell, significantly higher than the ones obtained for the other three cells (around 100).

When calculated, mean fiber length of each of the cells revealed no significant differences between the three of the cell lines: bEnd.3, BJ and MG-63 (Fig. 5). Only OL-93 cells show a small decrease in the mean fiber length as compared with the other cell lines.

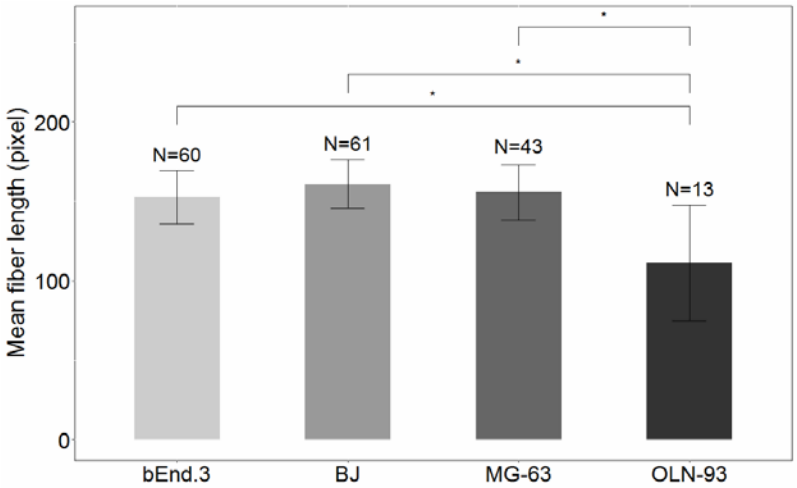

Fig. 5. Mean fiber length determined for the four types of cells. *N* represents the number of cells analyzed for each condition. The data were analyzed using one-way ANOVA with Fisher post-hoc tests with significance level: *$p < 0.05$.

CYTOSKELETON POLARIZATION

A more accurate classification of the four cell types was performed through the study of the actin filaments polarization (Fig. 6).

The polarity values measured for bEnd.3 cells vary between 0.01 and 0.65, with the most frequent values around 0.3. The same interval of variation is observed for the BJ cells, although the most frequent values are around 0.6. Therefore, a higher mean polarity value is reported for BJ cells. For the MG-63 and OLN-93 cells, smaller polarity values were computed. A small number of cells reach extreme polarity values. Most of the values for MG-63 vary between 0.01 and 0.08, with a peak at the 0.08 value. However, a smaller population is reported around 0.16. OLN-93 cells polarity values vary between 0.06 and 0.18 and peak around the value of 0.11.

In the density distribution of polarity values, the shape indicates significant differences between most of cell lines (Fig. 7). Comparable variability is observed for the values of bEnd.3 and BJ cells, respectively of MG-63 and OLN-93 cells. In Fig. 8 we can see that there are significant differences between the polarity values computed for every cell, except between MG-63 and OLN-93 (around 0.1).

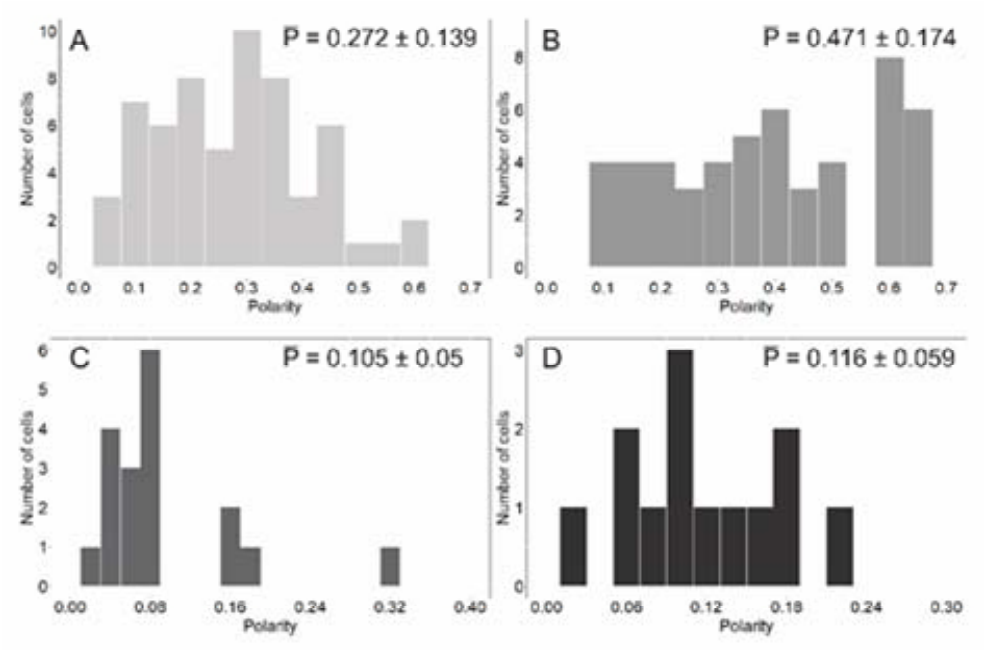

Fig. 6. Histogram for the number of cells against polarity values for (A) bEnd.3; (B) BJ; (C) MG-63; (D) OLN-93. $\bar{P}$ is reported as mean polarity ± SD.

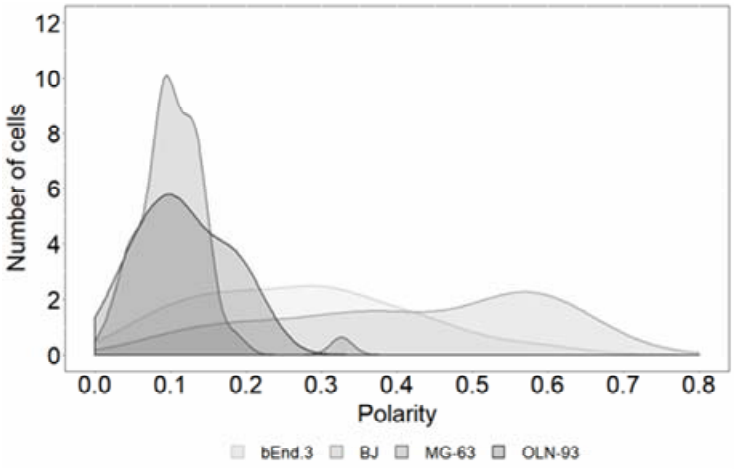

Fig. 7. Number of cells against polarity values of the four cell lines analyzed.

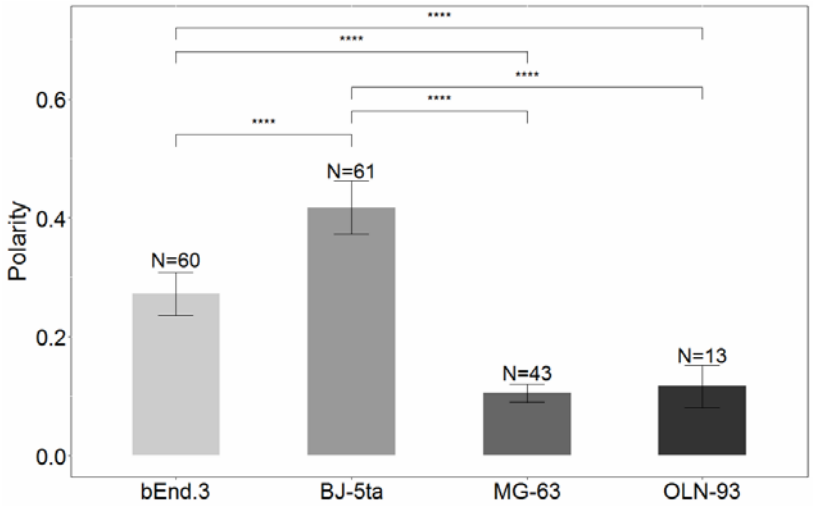

Fig. 8. Polarity determined for the four types of cells. *N* represents the number of cells analyzed for each condition. The data were analyzed using one-way ANOVA with Fisher post-hoc tests with significance level: **p* < 0.05; ***p* < 0.01; ****p* < 0.005; *****p* < 0.001.

CONCLUSION

The algorithm parameters were optimized and used to perform a comparative analysis between four types of cells. Significant differences between morphologies were revealed. Prior to processing, greater polarity, individual fiber length and number of fibers were reported for the BJ cell line. However, no significant difference was reported regarding mean fiber lengths.

The variation of the computational parameters enabled a precise detection of fiber structures. We adapted the FiberScore base algorithm and optimized the computational parameters in order to analyze different morphologies independently of the pixel intensity.

Among the studies addressing the morphology of the cellular cytoskeleton, it has been reported an extensive use of template-based detection methods for actin fibers. It has been observed that the physiological role of the cells is inducing preferential shapes and orientations in the actin cytoskeleton [6].

Starting from our results, a dynamic analysis of actin fibers conformational changes can be carried out. The algorithm feature that enables the efficient separation between the structures of interest and background proved useful even for images with lower quality. The consistency of the statistical analysis against the different cell types indicates that the algorithm can detect small conformational differences, fact that can be beneficial when studying physiological processes due to different treatments.

REFERENCES

1. HARVEY, L., B. ARNOLD, Z. LAWRENCE, M. PAUL, B. DAVID, D. JAMES, *Molecular Cell Biology*, 4th edition, W.H. Freeman, New York, 2000.
2. LICHTENSTEIN, N., B. GEIBER, Z. KAM, Quantitative analysis of cytoskeletal organization by digital fluorescent microscopy, *Cytometry A*, 2003, **54A**(1), 8–18.
3. PHAM, R.Q., *Detection of Curvilinear Objects Using a Template Based Comparison: Applications to Microscopy and Solar Images*, MSc, New Mexico State University, May 2013.
4. PITTEWAY, M., A. GREEN, Bresenham's algorithm with run line coding shortcut, *The Computer Journal*, 1982, **25**(1), 114–115.
5. STILES, J., C. AMAYA, R. PHAM, R. ROWNTREE, M. LACAZE, A. MULNE, BISCHOFF, J., KOKTA, V., BOUCHERON, L., MITCHELL, D., BRYAN, B., Propranolol treatment of infantile hemangioma endothelial cells: A molecular analysis, *Experimental and Therapeutic Medicine*, 2012, **4**(4), 594–604.
6. STILES, J., R. PHAM, R. ROWNTREE, C. AMAYA, J. BATTISTE, L. BOUCHERON, D. MITCHELL, B. BRYAN, Morphological restriction of human coronary artery endothelial cells substantially impacts global gene expression patterns, *The FEBS Journal*, 2013, **280**(18), 4474–4494.
7. SUETSUGU, S., T. TAKENAWA, Regulation of cortical actin networks in cell migration, *International Review of Cytology*, 2003, **229**, 245–286.
8. YOGURTCU, O., J. KIM, S. SUN, A mechanochemical model of actin filaments, *Biophysical Journal*, 2012, **103**(4), 719–727.
9. ***Cell polarity – Latest research and news, https://www.nature.com/subjects/cell-polarity.